The influence of precipitation weighting on interannual variability of stable water isotopes in Greenland

A. Persson,[1] P. L. Langen,[1] P. Ditlevsen,[1] and B. M. Vinther[1]

Received 17 December 2010; revised 12 July 2011; accepted 15 July 2011; published 26 October 2011.

[1] We investigate the effect of precipitation weighting on annual δ values of stable water isotopes in ice cores from Greenland. This effect can explain the observation from ice cores that δ values in northwestern Greenland are less related to annual coastal temperatures than are the δ values in southern and central Greenland ice cores. Furthermore, the precipitation weighting can explain the result of Vinther et al. (2010) that exclusion of summer layers increases information about annual temperature in Greenland ice core records. We study these effects by comparing arithmetic annual means of a regional temperature signal to annual means of the same signal weighted by local precipitation. Specifically, we apply the ERA-40 reanalysis of meteorological observations to compute time series of southwest Greenland temperatures in annual means and in annual precipitation weighted means. We find that the correlation between these temperature series is highest in southern Greenland, decreasing toward the north, and that the correlation is controlled by the seasonal time scale precipitation weighting. A statistical model is developed to understand the role of climatic parameters in this correlation. The low correlation in northwestern Greenland is caused in equal parts by a relatively lower mean fraction of precipitation during winter in this sector and a larger year-to-year variability of this fraction.

Citation: Persson, A., P. L. Langen, P. Ditlevsen, and B. M. Vinther (2011), The influence of precipitation weighting on interannual variability of stable water isotopes in Greenland, *J. Geophys. Res.*, *116*, D20120, doi:10.1029/2010JD015517.

1. Introduction

[2] The isotopic composition of the water contained in the ice sheets compared to that of the ocean (usually given by $\delta^{18}O$ and δD, collectively referred to here as δ) is considered a proxy for the atmospheric temperature at the time of deposition [*Dansgaard*, 1964]. As a moist air mass is advected above the ice sheet, precipitation will continuously deplete the δ value of the remaining vapor. This isotopic distillation is in the simplest picture controlled by the difference between the condensation temperature and the temperature at which condensation first occurred [*Dansgaard*, 1964]. However, the fractionation factors, and cloud processes such as the switching from liquid to solid droplets do depend on temperature directly [*Ciais and Jouzel*, 1994]. Several other factors can complicate the interpretation of δ as a record of paleotemperature. The condensation temperature may not always be strongly related to the surface air temperature due to variations of both the transport level and the strength of the near-surface temperature inversion during winter. A change in source region location or conditions will alter the initial dew point of the air mass and initial vapor δ. The locations of the source regions depend on the atmospheric circulation, which is also related to the level of transport. At the surface, snow drifting can corrupt the local signal [*Fisher et al.*, 1985]. Even after the final deposition, exchange of water vapor with the surrounding firn layers [*Johnsen*, 1977] and possibly the atmosphere [*Town et al.*, 2008] can still modify the isotopic signal. Another limitation of δ as a temperature proxy is that it is only recorded when snow is deposited on the ice sheet. It is thus a record dependent on the local conditions of precipitation [*Steig et al.*, 1994].

[3] Despite these complicating factors an approximately linear relationship between the depletion of heavy water isotopes and temperature is observed in polar regions for both spatial and temporal variability, although with a different slope [e.g., *Capron et al.* 2010].

[4] Due to their accurate dating [*Vinther et al.*, 2006], the Greenland ice core records potentially provide information on atmospheric circulation and regional temperature in near annual resolution [*Barlow et al.*, 1993; *Rogers et al.*, 1998; *Vinther*, 2003; *Schneider and Noone*, 2007; *Steen-Larsen et al.*, 2011]. This information can supplement the instrumental observations which are limited to recent centuries, but a further understanding of the year-to-year temperature-δ relationship is still needed. We address two specific observations:

[5] 1. In south and central Greenland, studies have found a high correlation between annual values of δ and temperature

[1]Centre for Ice and Climate, Niels Bohr Institute, University of Copenhagen, Copenhagen, Denmark.

0148-0227/11/2010JD015517

Table 1. Ice Cores

	Ice Cores							ERA-40	
Drill Site	Latitude (°N)	Longitude (°W)	Elevation (m a.s.l.)	Time Span	Stack	Accumulation Rate[a] (m ice/yr)	Accumulation Rate[b] 1957– (m ice/yr)	Accumulation Rate (m ice/yr)	Standard Deviation of Accumulation (m ice/yr)
DYE-3 71	65.18	43.83	2480	1239–1971	DYE-3	0.56	0.58[c]	0.78	0.12
DYE-3 79	65.18	43.83	2480	BC–1979b	DYE-3	0.56	0.58[c]	0.78	0.12
DYE-3 4B	65.17	43.93	2491	1691–1983	DYE-3	0.535	0.57[d]	0.76	0.12
DYE-3 18C	65.03	44.39	2620	1776–1984	DYE-3	0.44	0.44[d]	0.67	0.10
DYE-3 20D	65.00	44.45	2625	1767–1984	DYE-3	0.44	0.42[d]	0.66	0.10
GRIP 89-1	72.58	37.64	3238	918–1989	GRIP	0.23	0.21[c]	0.14	0.03
GRIP 89-2	72.58	37.64	3238	1772–1989	GRIP	0.23	0.21[c]	0.14	0.03
GRIP 89-3	72.58	37.64	3238	BC–1989b	GRIP	0.23	0.21[c]	0.14	0.03
GRIP 91	72.58	37.64	3238	1721–1991	GRIP	0.23	0.21[c]	0.14	0.03
GRIP 92	72.58	37.64	3238	1622–1992	GRIP	0.23	0.21[c]	0.14	0.03
GRIP 93	72.58	37.64	3238	1062–1993	GRIP	0.23	0.21[c]	0.14	0.03
Camp Century 1	77.18	61.11	1880	1761–1977	CC	0.38	0.35[e]	0.31	0.07
Camp Century 2	77.22	60.80	1910	1839–1977	CC	0.38	0.35[e]	0.31	0.07
GISP2-D	72.60	38.50	3200	1270–1989	No	0.245	0.23[e]	0.15	0.03
Crête	71.12	37.32	3172	551–1974	No	0.289	0.29[c]	0.20	0.04
Milcent	70.30	44.50	2410	1173–1973	No	0.54	0.50[c]	0.44	0.07
Renland	71.27	26.73	2350	BC–1988b	No	0.50	0.50[d]	0.41	0.10
Site A	70.63	35.82	3092	1622–1985	No	0.292	0.29[d]	0.24	0.05
Site B	70.65	37.48	3138	1716–1984	No	0.306	0.30[d]	0.21	0.04
Site D	70.64	39.62	3018	1766–1984	No	0.354	0.34[d]	0.26	0.04
Site E	71.76	35.85	3087	1722–1985	No	0.215	0.21[d]	0.17	0.03
Site G	71.15	35.84	3098	1776–1985	No	0.249	0.24[d]	0.21	0.04
NEEM 07S3	77.45	51.06	2484	1738–2005	No	0.22	0.21[f]	0.18	0.04

[a]Published estimates of present-day accumulation from *Clausen and Hammer* [1988], *Steen-Larsen et al.* [2011], and *Vinther et al.* [2010] and references therein.
[b]Calculated mean annual accumulation in the period of overlap between the ice core and ERA-40. Density profiles or annual accumulation data are taken from the listed sources.
[c]*Andersen et al.* [2006].
[d]*Vinther et al.* [2010].
[e]*Cuffey and Clow* [1997].
[f]B. Vinther, unpublished data, 2011.

measurements from the southwest coast of Greenland over the last centuries [e.g., *White et al.*, 1997; *Vinther et al.*, 2010]. In contrast, the Camp Century records, from northwest Greenland, are only weakly related to the southwest coast temperature (see section 2.1).

[6] 2. In a recent study, *Vinther et al.* [2010] compared south and central Greenland ice core records of $\delta^{18}O$ in subannual resolution with temperatures observed at the coast. It was demonstrated that the winter layers rather than the summer layers contain more information about the temperature. In fact, the optimal correlation between δ values and annual temperature was obtained using only 50% of each annual layer centered on the winter minimum. The exclusion of summer layers therefore increases the information about the annual temperature.

[7] Here we investigate if these two observations can be attributed to the seasonal timing of precipitation. Year-to-year variability of the seasonal timing has a large potential impact on the δ value recorded by an ice core, because the interannual variability of δ is small compared to variability at shorter time scales, such as the annual cycle. Neglecting other processes, we assess the separate effect of this precipitation weighting on the present-day temperature-δ relationship in Greenland. Specifically we quantify the effect of precipitation weighting on the pure temperature signal.

[8] Due to the limited spatial and temporal coverage of direct meteorological observations in this region, temperature and precipitation are taken from the ERA-40 reanalysis [*Uppala et al.*, 2005], which covers the period 1957–2002. We apply the methodology of *Sime et al.* [2009] to evaluate the relative importance of the synoptic and seasonal scale variability of the precipitation. We further develop a simple statistical model for the seasonal scale precipitation intermittency to identify the key mechanisms altering the original temperature signal. Using these tools, the implied signal loss can be mapped over Greenland and compared to the correlations between measurements of annual δ values in ice cores and coastal temperature.

2. Data

2.1. Ice Cores

[9] We use isotope data from 23 ice cores at 16 different locations in Greenland (see Table 1 and Figure 1). Annual δ values of heavy water isotopes are taken by *Vinther et al.* [2010]. Additionally two shallow ice cores from Camp Century [*Clausen and Hammer*, 1988] and a shallow core from the North Greenland Eemian Ice Drilling (NEEM) site [*Steen-Larsen et al.*, 2011] are included in this study. All the records are of $\delta^{18}O$ with the exception of the GISP2 record, where δD has been measured. In summary, the annual δ series have been constructed as follows (for a complete description, see *Vinther et al.* [2010]). Each record is corrected for diffusion of water vapor in the firn which

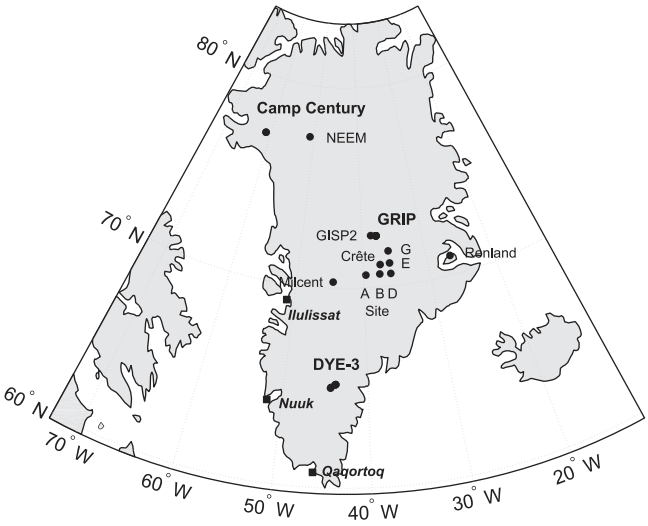

Figure 1. Map of Greenland with the drill sites of the cores included in the present study (circles) and the three observation sites (squares) included in the southwest Greenland temperature record [*Vinther et al.*, 2006].

dampens the annual cycle of the δ signal [*Johnsen et al.*, 2000]. Summer maxima are then identified in the records and the annual summer-to-summer mean δ time series for each core is calculated.

[10] For the period of overlap, δ values from the ice cores can be compared directly with the temperature measurements from the coast of Greenland. Sufficiently long series of measurements are available only from southwestern Greenland, where a combined temperature record has been compiled reaching back to 1784 AD [*Vinther et al.*, 2006]. This record is a composite of three local records from Ilulissat, Nuuk and Qaqortoq. The δ values from each site and the combined southwest record (hereafter referred to as T^{SW}) cannot be directly compared, because the cores have different stratigraphic noise levels depending on the conditions at the site [*Fisher et al.*, 1985]. This noise is caused mainly by the formation of sastrugi.

[11] However, as is described in Appendix A, if the signal-to-noise ratio (SNR) of the ice core δ signal is known, then the correlation between δ and T^{SW} can to some extent be corrected for the stratigraphic noise. At the three sites with multiple cores the SNR can be directly calculated. For the period where all cores have data (1841–1970), we calculate the corrected correlation between the common annual δ signal and T^{SW} to be 0.19 ± 0.09 at Camp Century (northwest), 0.60 ± 0.06 at GRIP (Summit) and 0.63 ± 0.05 at DYE-3 (south).

2.2. ERA-40

[12] We use daily precipitation and 2 meter air temperature from the ERA-40 reanalysis of meteorological observations by the European Centre for Medium-Range Forecasts [*Uppala et al.*, 2005]. ERA-40 covers the period from September 1957 to August 2002 and assimilates data from a variety of sources. The available sources change throughout the period, but most notable is the inclusion of satellite data from 1979 onward.

[13] Several studies have successfully used the precipitation fields from ERA-40 in Greenland. *Sodemann et al.* [2008a] diagnosed the moisture sources of the Greenland ice sheet by applying a back trajectory analysis to the ERA-40 reanalysis. Applying the zero-dimensional Mixed Cloud Isotope Model [*Ciais and Jouzel*, 1994] to the individual trajectories, a significant North Atlantic Oscillation imprint was found in the modeled δ values over most of Greenland [*Sodemann et al.*, 2008b] in agreement with observations from Greenland ice cores [e.g., *White et al.*, 1997; *Vinther et al.*, 2010]. In a different study, *Schuenemann and Cassano* [2009] used a synoptic climatology of ERA-40 surface pressure as a benchmark to select the best AR4 regional models to investigate future changes in accumulation rates. The subannual climatology of precipitation over the Greenland Ice Sheet of ERA-40 was also investigated in great detail by *Schuenemann et al.* [2009]. Finally, ERA-40 has been used to quantify the effect of precipitation weighting over the Antarctic Peninsula [*Sime et al.*, 2009].

[14] While the ERA-40 reanalysis is generally considered more reliable in the Arctic than in the Antarctic especially prior to 1979 [*Bromwich et al.*, 2007], there is a lack of meteorological stations and reliable measurements of snow accumulation over the Greenland Ice Sheet to validate the reanalysis in this region. Instead Table 1 allows comparison of annual mean accumulation rates from ERA-40 and those determined from the ice cores used in this study. We have estimated the accumulation rate using only the annual layers, which are contained in the ERA-40 period from density profiles and previously published annual accumulation reconstructions [*Andersen et al.*, 2006; *Cuffey and Clow*, 1997; *Vinther et al.*, 2010]. It should be noted that the majority of the cores used in the present study, only have a limited overlap with ERA-40. In a detailed study, *Hanna et al.* [2006] compared annual accumulation from ERA-40 to 58 ice core accumulation data sets finding a mean annual correlation of 0.53. Because the annual layers contain noise from snow drift this does not clearly quantify the accuracy of ERA-40, but at least a significant correlation is observed. Furthermore, *Hanna et al.* [2006] found southern Greenland to be too wet and northern Greenland too dry, which can also be concluded from Table 1. This has no direct implications for the present study, since the total annual accumulation does not affect the annual precipitation weighted temperature directly. Instead the precipitation weighted temperature is fully determined by the relative distribution of precipitation across the year. Unfortunately, no sufficiently long records of precipitation from interior Greenland are available to validate the subannual climatology of ERA-40 precipitation over the Greenland Ice Sheet.

2.3. REMO$_{iso}$

[15] We include modeled isotope fractions in precipitation from REMO$_{iso}$, a regional circulation model with isotopic tracers [see *Sjolte et al.*, 2011]. Boundary conditions for this model are provided by the European Centre/Hamburg global isotopic general circulation model (ECHAM4) [*Hoffmann et al.*, 1998]. In both the regional and global model, the upper wind field is relaxed toward the values of ERA-40 using a nudging technique described by *von Storch*

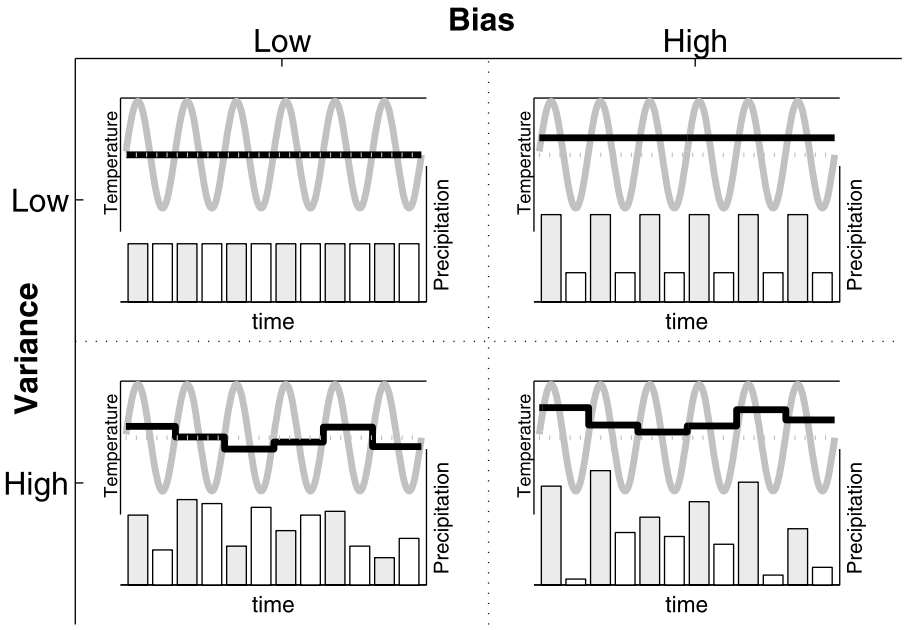

Figure 2. A periodic temperature variation (gray solid lines) sampled using different patterns of precipitation (histograms). Depending on the statistics of the precipitation, the resulting precipitation-weighted temperature (black lines) is biased and/or has induced variability. The period can be considered as the annual cycle, but the principles involved apply to any time scale on which the temperature varies.

et al. [2000]. The δ values from REMO$_{iso}$ are used in section 5.1.3 to investigate the statistical similarity between the annual temperature and δ cycle.

3. Precipitation-Weighted Temperatures

[16] To quantify the impact of precipitation timing, we examine the degree to which the (time-weighted) annual mean temperature

$$T_a = \frac{1}{N}\sum_{j=1}^{N} T_j \tag{1}$$

is represented by the precipitation weighted annual mean temperature

$$T_{pw} = \frac{\sum_{j=1}^{N} T_j p_j}{\sum_{j=1}^{N} p_j}. \tag{2}$$

In the above equations N is the number of time-equidistant samples (days) that are used per year. T_j and p_j denote the mean temperature and precipitation rate, respectively, in the jth time interval. The mean annual temperature is typically the climate parameter we are interested in while the precipitation weighted temperature is the parameter we will be able to extract from a record which is deposited at a rate proportional to precipitation. Even if the relation between δ and temperature is perfect at the time of deposition, the correlation between T_a and T_{pw} still sets the upper limit for the temperature information contained directly in the isotope record. The use of T_{pw} as an analogy to sampling δ in ice cores therefore provides a simple framework for quantifying the effect of the precipitation weighting separately.

[17] Because the interannual variability of temperature is small compared to variability at shorter time scales, such as the annual cycle, uneven sampling will bias the precipitation weighted temperature. Figure 2 illustrates the two different effects of the precipitation on the record. Firstly, precipitation weighting can shift the mean value of T_{pw} if the local weather conditions are such that the amount of precipitation depends on the temperature. Say if the climatic conditions change, such that the mean seasonality of the precipitation changes, there would be a systematic biasing due to the changing weighting of warm summers and cold winters, even without a true change in temperature (Figure 2, right). The important aspect of mean biasing has undergone thorough investigation [e.g., *Werner et al.*, 2000; *Masson-Delmotte et al.*, 2005; *Sime et al.*, 2008; *Langen and Vinther*, 2009]. Secondly, the stochastic nature of the deposition can induce an artificial variability in the record thereby degrading the interannual temperature signal therein. A warm year may for instance have a high value of T_{pw}, but it may also have a low value if, by chance, more precipitation should fall during winter (Figure 2, bottom). In the present study we focus on the second aspect, and specifically the present-day correlation between T_a and T_{pw}.

[18] In principle, year-to-year variability of T_{pw} can be induced by precipitation intermittency at any subannual time scale on which the temperature varies. To determine the important time scales the methodology of *Sime et al.* [2009] has also been applied at Greenland ice core sites. In this method the precipitation and temperature fields of ERA-40 are decomposed into frequency bands. For each band, the biasing of the annual temperature associated with the precipitation weighting can then be analyzed. In Greenland we find that the present-day correlation between T_a and T_{pw} is controlled by precipitation weighting at seasonal time

scales. Details of the method and the analysis are shown in Appendix B.

[19] The local annual mean and precipitation weighted annual mean temperatures can be calculated directly using equations (1) and (2). This has been done year by year (summer to summer) for the period 1958–2002 giving 44 points. At all sites, but at GRIP in particular, the correlations between T_a and T_{pw} using the local surface temperatures are much lower than the correlations between observed δ and T^{SW} (e.g.,. at GRIP the former is 0.27 and the latter is 0.60 at GRIP). However, it may not be meaningful to compare these values, since the annual surface temperature in central Greenland is dominated by the local strength of the temperature inversion, which develops in periods with limited accumulation. In contrast, temperature inversions have less impact on the annual δ signal and T^{SW}.

3.1. The Choice of Temperature Cycle

[20] To investigate the effect of precipitation weighting on the relationship between coastal temperature and recorded δ values in the interior of Greenland, we determine how the precipitation weighting affects the coastal temperature signal. The idea is that by quantifying the signal loss in the ideal case where the recorded δ value in the ice cores is proportional to the coastal temperature, we determine an upper limit for the information about coastal temperature contained in the ice core.

[21] A study by *Steffensen* [1985] confirms that the subannual δ values could be related to coastal temperatures. By weighting temperatures from south Greenland with the observed local precipitation at DYE-3, this study found a detailed correspondence in subannual resolution with the δ signal recorded in a snow pit there. In effect, the ice core is sampling the coastal temperatures whenever moist air is advected to the site. This conclusion is also partly supported by a model study by *Werner and Heimann* [2002], which reported the δ signal of the Summit area to integrate the climatic history of a broader region and to be more related to the temperature at the southwest coast weighted by Summit precipitation than to T_{pw} at Summit.

[22] Following such an approach, it is possible to evaluate the effect of the precipitation weighting separately, by making the simplifying assumption that the relevant temperature signal has the same annual cycle all over the Greenland Ice Sheet (except for the mean, which is irrelevant for this study). At each site we therefore use local information about precipitation to construct a precipitation weighted series of southwest Greenland temperature, T_{pw}^{SW}, and compare it to the unweighted T_a^{SW}. A further comparison between the seasonal cycles of T^{SW} and δ will be made in section 5.1.3. To facilitate comparison with the *Vinther et al.* [2010] analysis, T^{SW} is calculated, in ERA-40, as the mean of surface air temperatures at Illulissat, Nuuk and Qaqortoq. Except at Camp Century, the correlations between T_a^{SW} and T_{pw}^{SW} are higher (DYE-3 0.69 ± 0.08, GRIP 0.66 ± 0.09 and Camp Century −0.04 ± 0.15) than the correlations calculated using local temperatures.

3.2. Winter Temperature Control on Annual Temperature

[23] In temperature observations from the southwest coast of Greenland [*Vinther et al.*, 2006] the standard deviation of the summer half year (defined here as May–October) and winter half year (November–April) are 1.0 K and 2.3 K, respectively. Since winters and summers enter with equal weights in the time average, the larger winter variability leads to annual mean temperature variations being dominated by the winter signal. Indeed the correlation between the annual mean temperature and the summer and winter half-year temperatures is 0.80 and 0.96, respectively. In both cases, the calculation of the annual mean is centered around the season in question, i.e., February–January for summer and August–July for winter values. The correlation between half year temperatures is higher in winters than in summers, which we find to be the case all over Greenland. The conclusion is that summers tend to be similar while winters differ more and it is thus the winter that determines whether a year will be warm or cold. Consequently, annual averages should be taken as summer to summer rather than following the calendar winter to winter when studying interannual variability. Winter-to-winter averages tend to mix the signal between two winters while a summer-to-summer average spans a single winter.

4. The Statistical Model

[24] To address the problems posed in the introduction, we develop a simple statistical model for the effect of precipitation weighting based on the observations discussed in section 3.2. These observations suggest that the correlation between T_a^{SW} and T_{pw}^{SW} is determined mainly by precipitation intermittency on seasonal time scales and that the interannual variability of the summer temperature can be ignored. The statistical model allows identification of the statistical properties that characterize the loss of information associated with the seasonal precipitation weighting and their spatial variability.

[25] We calculate the correlation between time and precipitation weighted annual means of a general signal, T, with an annual cycle qualitatively similar to T^{SW}. Expanding (2), T_{pw} can be split into contributions from summer and winter events

$$T_{pw,i} = \left(\sum_j p_j\right)^{-1} \left(\sum_{j\in\text{summer } i} p_j T_j + \sum_{j\in\text{winter } i} p_j T_j\right) \qquad (3)$$

where p_j and T_j denote the precipitation and temperature of event j, respectively, and i is the year. Since the previous analysis suggests that the correlation between T and T_{pw} is limited mainly by precipitation weighting on the seasonal time scale, we therefore neglect temperature variability on shorter time scales and thus assume the temperature throughout each season to be time constant. Furthermore, the interannual variability of the summer temperature is ignored since it is much smaller than that of winter. Using these assumptions (3) reduces to

$$T_{pw,i} = x_i W_i + (1 - x_i) S \qquad (4)$$

where for each year i, x_i is the fraction of the total precipitation falling during winter, W_i is the mean winter temperature and

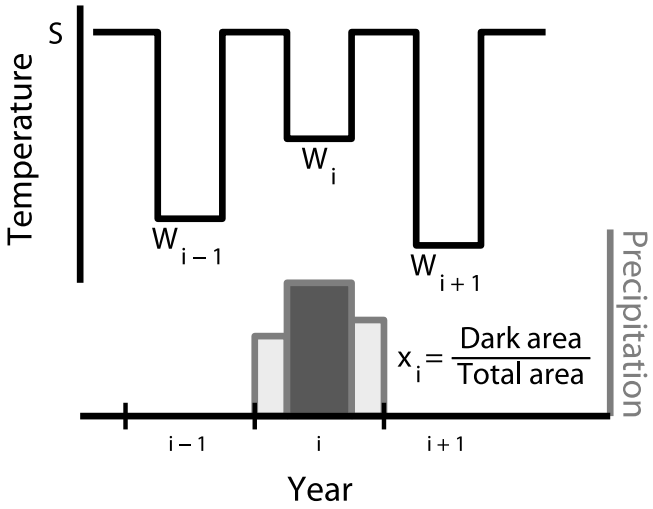

Figure 3. The statistical model. Summer half-year temperature, *S*, has no interannual variability, unlike winter half-year temperatures, *W*, and the winter fraction of precipitation, *x*.

S is the constant summer temperature (see Figure 3). In terms of these quantities the annual mean temperature is simply

$$T_{a,i} = \beta W_i + (1-\beta)S \tag{5}$$

where the constant β is the fraction of the year defined as winter. Note that the difference between T_{pw} and T_a is then that the constant factor β takes the place of x_i. Together (4) and (5) form our statistical model. We treat x_i and W_i as annual stochastic variables with mean and variance determined from either observations or circulation models. The correlation between T_a and T_{pw} can now be directly calculated by first calculating their covariance and respective variances (see Appendix C):

$$\overline{T_a' T_{pw}'} = \beta\left(\bar{x}\sigma_W^2 - \sigma_{x,W}\left(S - \overline{W}\right)\right) \tag{6}$$

$$\overline{T_a'^2} = \beta^2 \sigma_W^2 \tag{7}$$

$$\overline{T_{pw}'^2} \approx \bar{x}^2\sigma_W^2 + \left(S-\overline{W}\right)^2\sigma_x^2 - 2c_{x,W}\sigma_x\sigma_W\bar{x}\left(S-\overline{W}\right). \tag{8}$$

Here σ denotes standard deviation and $c_{x,W}$ is the coefficient of linear correlation between x and W, which measures the tendency for warm (cold) winters to have high (low) precipitation relative to summer. Let us first interpret the terms in the variance of T_{pw} (8). The two first terms can be identified as the variance induced by the interannual variability of the temperature and the seasonality of precipitation, respectively. The former can thus be considered as the power of the signal we are trying to extract, and the latter as the power of the noise caused by the precipitation weighting, i.e., the variance of T_{pw} provided T_a is constant. The third term arises from the tendency for cold years to under (over) sample winters for positive (negative) $c_{x,W}$ thereby damping (amplifying) the temperature signal. Finally we get

$$c_{T_a,T_{pw}} \equiv \frac{\overline{T_a' T_{pw}'}}{\left(\overline{T_a'^2}\,\overline{T_{pw}'^2}\right)^{\frac{1}{2}}} \approx \frac{1 - f c_{x,W}}{\left(1 + f^2 - 2f c_{x,W}\right)^{\frac{1}{2}}} \tag{9}$$

with the following notation introduced

$$f \equiv \frac{\tilde{\sigma}_x}{\tilde{\sigma}_W} \tag{10}$$

$$\tilde{\sigma}_W \equiv \frac{\sigma_W}{S - \overline{W}} \tag{11}$$

$$\tilde{\sigma}_x \equiv \frac{\sigma_x}{\bar{x}} \tag{12}$$

$\tilde{\sigma}_W$ and $\tilde{\sigma}_x$ are dimensionless measures of the strength of the interannual temperature signal and the precipitation weighting, respectively. Their ratio, *f*, then measures the dominance of the precipitation weighting. $c_{Ta,Tpw}$ is seen to be monotonically decreasing with both $c_{x,W}$ and *f*. These quantities represent the two different characteristics of the seasonal precipitation weighting that imply a corruption of the annual signal: a systematical oversampling of warm winters and a larger variability of the noise induced in T_{pw} by the precipitation weighting. The analogy to signal analysis is apparent if we think of T_{pw} as a corrupted version of T_a. In the case that winter temperatures and winter ratios of precipitation are independent, $c_{x,W} = 0, f^2$ is indeed equal to one over the signal to noise ratio and (9) reduces to the well known formula

$$c_{T_a,T_{pw}} = \frac{1}{(1+f^2)^{\frac{1}{2}}} \tag{13}$$

5. Regional Variability of the Precipitation Weighting

[26] Using the simple statistical model developed in section 4, regional differences of the seasonal precipitation weighting can be investigated. The model parameters *f* and $c_{x,W}$ are determined locally using T^{SW} and precipitation from ERA-40.

5.1. Statistical Model Parameters Estimated From ERA-40

[27] The interannual winter temperature variability relative to the amplitude of the annual cycle, $\tilde{\sigma}_W$, is calculated from ERA-40 T^{SW} to be 0.17. Figures 4a and 4b show maps of the standard deviation, σ_x, and the mean, $\bar{x}$, of the winter fraction of annual precipitation over Greenland. Their ratio $\tilde{\sigma}_x$ is proportional to *f*, since a spatially constant temperature signal is used. Panel c shows *f*, which is seen to have a value slightly below one in southeastern Greenland, indicating that the temperature signal here is stronger than the noise from the seasonal precipitation weighting. A northwestern spatial gradient of *f* is seen and the value of *f* is three times larger in the northwesternmost part relative to the southeastern part of Greenland. As can be seen in panel a and b this regional difference is caused in equal parts by a higher σ_x and a lower $\bar{x}$. The low value of $\bar{x}$ in northwest Greenland is due to a lower absolute amount of winter precipitation here (not shown). Panel d shows $c_{x,W}$ calculated from ERA-40. This correlation has a significant (at 5% level) positive value in northwestern Greenland (~0.4) reducing the gradient between T_a^{SW} and T_{pw}^{SW} thereby masking the temperature

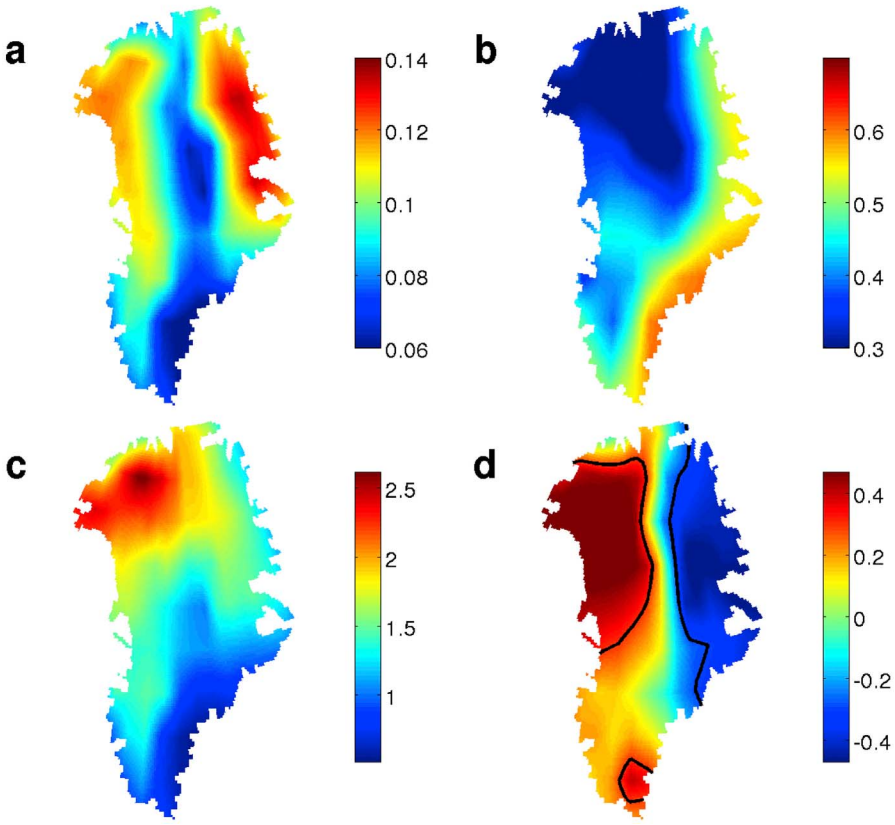

Figure 4. Parameters of the statistical model (equation (9)) calculated using the local precipitation fields and southwest Greenland surface air temperature from ERA-40. (a) σ_x, (b) $\bar{x}$, (c) $f = (\sigma_x/\bar{x})/\tilde{\sigma}_W$, and (d) $c_{x,W}$. The black line marks areas where the correlation is significantly different from zero (5% level).

signal further here. A similar in magnitude, but negative correlation is observed in northeastern Greenland. A small area of significant positive correlation is also seen at the southern tip of Greenland.

[28] Figures 5a–5c show maps of $c_{T_a^{SW},T_{pw}^{SW}}$ as calculated from daily ERA-40 fields, the statistical model (equation (9)) with f and $c_{x,W}$ determined from ERA-40, and the simplified statistical model (equation (13)), which assumes $c_{x,W} = 0$. Comparing Figures 5a and 5c, it is seen that the simplified statistical model captures the main feature of Figure 5a that the correlation between T_a^{SW} and T_{pw}^{SW} decreases as one moves to the northwest. The statistical model performs even better when the covariance of x and W is taken into account (Figure 5b). Considering the strong simplifying assumptions imposed on the statistical model, i.e., the two-step seasonal cycle, the constant summer temperature and the constant duration of winter, it fits the correlations calculated from the daily ERA-40 fields remarkably well.

[29] Similar to the Camp Century δ records, T_{pw}^{SW} in northwestern Greenland is at most weakly related to T_a^{SW}, but before a further comparison can be made, some issues with the results of this section must be addressed.

5.1.1. Parameter Uncertainty

[30] To investigate if the regional differences of the parameters of the statistical model are valid beyond the particular 44 years of ERA-40, the parameters have been calculated repeatedly using 44 randomly selected years (with replacement). We evaluate the relative uncertainty in f to be approximately 15% (with a significant spatial positive correlation of the error). As f increases by a factor of three in northwest Greenland, the spatial gradient of f is therefore robust.

[31] To rule out the effect of additional inaccuracies in ERA-40 prior to the inclusion of satellites, f has been recalculated using only data from the satellite period. Although a slightly (~20%) lower spatial gradient of f is then observed, the difference is within the expected when halving the number of observations. When using only data from the satellite period, f is still minimum in the northwest.

[32] As can be seen in Figure 4c the estimated $c_{x,W}$ has a clear east-west gradient. Even though $c_{x,W}$ provides an important correction to our interpretation of ERA-40 data, this correlation could be different for the relationship between local δ and x, particularly in eastern Greenland where the influence of T^{SW} is most likely reduced.

5.1.2. Limitations of Modeled Precipitation

[33] We do not expect ERA-40 to provide an exact history of the precipitation. Indeed we find no significant year-to-year correlation between T_{pw}^{SW} from ERA-40 and δ at DYE-3, GRIP or Camp Century, although a limited time overlap is available. However, the strength of the present study is that it does not depend explicitly on the precipitation history, but rather on its statistical properties, which we expect to be

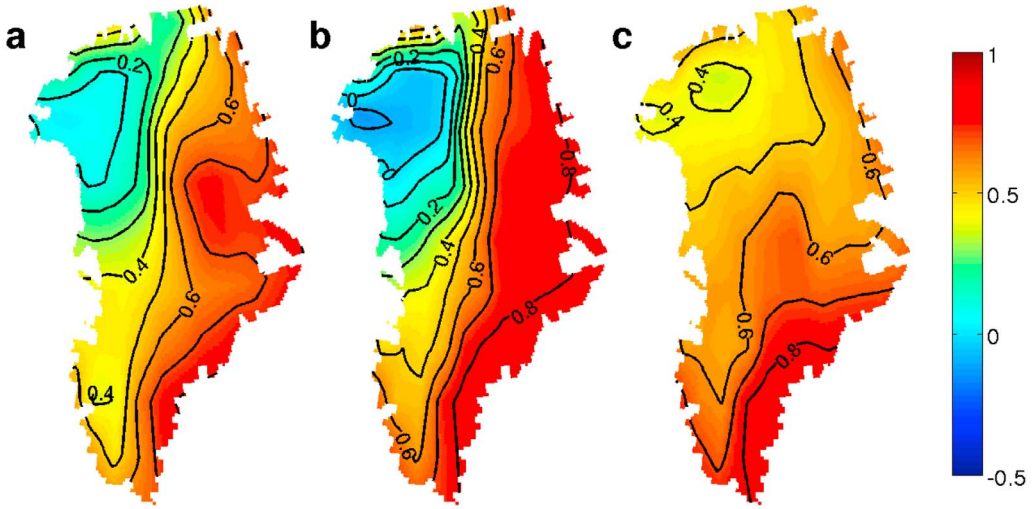

Figure 5. Coefficient of the correlation between southwest Greenland temperatures in annual mean, T_a^{SW}, and in precipitation-weighted mean, T_{pw}^{SW}. The correlations are calculated from ERA-40 using (a) daily temperatures and precipitation sums, (b) the statistical model (equation (9)), and (c) the simplified statistical model, which assumes winter temperature and winter fraction of precipitation to be uncorrelated (see equation (13)).

more reliable. To evaluate if the statistical model parameters in northwestern Greenland derived from ERA-40 are realistic, we compare to observations from meteorological stations at the coast. We use data from Upernavik [*Cappelen et al.*, 2008], the nearest Danish Meteorological Institute (DMI) station to Camp Century. Using the 67 years with complete data in the period 1890–1979, we find $\overline{x}$ = 0.39 (compared to 0.39 from ERA-40), σ_x = 0.11 (0.11) and $c_{x,W}$ = 0.06 (0.36) using local temperatures. The detailed similarity of $\overline{x}$ and σ_x is probably a coincidence, but it shows that the high values of $\tilde{\sigma}_x$ in northwestern Greenland simulated by ERA-40 are not unrealistic. ERA-40 still predicts a slightly higher value further north and inland, but no observations are available here. Contrary to the simulations of ERA-40, we find no significant correlation between x and W in the meteorological observations from any of the DMI stations on the west coast of Greenland. This indicates that such a correlation could be an artefact in ERA-40. The simplified statistical model for the loss of signal by precipitation weighting (13) is therefore preferable to equation (9) as the former does not include $c_{x,W}$.

5.1.3. The Annual Temperature Versus Annual δ Cycle

[34] The statistical model formulated in section 4 quantifies the loss of annual information when an underlying seasonal signal is recorded with a stochastic seasonal biasing. So far we have considered the effect of precipitation weighting on the spatially homogenous temperature field given by, T^{SW}. As already mentioned, the idea is that the maximum information about T^{SW} allowed in a δ record is determined by the limiting condition that the ice core samples a signal equal to T^{SW}. However, this argument is only valid provided that the inter annual variability of the seasonal cycles of T^{SW} and δ have similar statistics. Hence the summer snow δ should also be only weakly related to annual temperature and the interannual variability of the winter value relative to the amplitude of the annual cycle should not be larger for δ than for T^{SW}.

[35] We investigate the seasonal δ cycle using REMO$_{iso}$. A time series of monthly mean time-weighted δ is constructed, at each point, as the mean δ value of all precipitation events in that month (using equal weights). We find that this signal has statistics nearly identical to T^{SW}. The variance of summer means is on average only 25% of that of winter means and the analogue to $\tilde{\sigma}_W$, namely winter variance divided by the mean annual cycle has a mean value of $\tilde{\sigma}_\delta$ = 0.18 (for T^{SW} we found $\tilde{\sigma}_W$ = 0.17). This value is remarkably constant all over the Greenland Ice Sheet having excursions below 0.15 only in northeastern Greenland (minimum 0.10) and excursions above 0.23 only near the southeast coast. At the ice core sites we find 0.26 at DYE-3, 0.18 at GRIP and 0.19 at Camp Century indicating that spatial variability of $f_\delta \equiv \tilde{\sigma}_x/\tilde{\sigma}_\delta$ is controlled by $\tilde{\sigma}_x$ at least in the area of the drill sites included in the present study (except maybe Renland).

5.2. Comparison With Ice Cores

[36] As already shown, the weak relationship between δ and T_a^{SW} observed on annual time scales at Camp Century in northwestern Greenland is an expected result of the characteristics of precipitation in this region. To test if correlations between δ and T_a^{SW} are generally limited by seasonal precipitation intermittency, we compare the results of the statistical model to ice core observations. However, before such a comparison is possible, $c_{\delta,T^{SW}}$ must be corrected for stratigraphic noise as shown in Appendix A, using the local signal-to-noise ratio, SNR. Unfortunately, this correction is most important at sites where only one core is available and the SNR cannot be calculated directly. An explicit dependency of the SNR on latitude was suggested by *Fisher et al.* [1985] consisting of a steadily increasing noise with latitude combined with a stronger common signal in the north. Taking a similar approach we therefore estimate the SNR at each site with values linearly interpolated between the three sites with known SNR using the latitude; see Figure 6b (inset). Using these estimates of SNR, the corrected $c_{\delta,T^{SW}}$

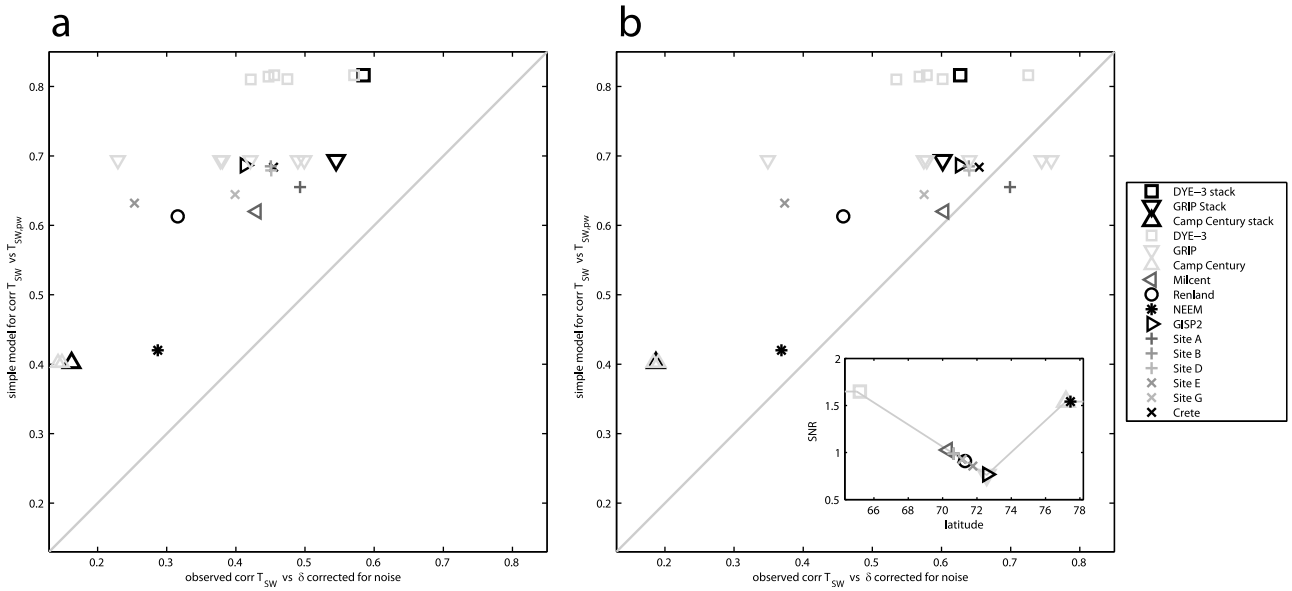

Figure 6. (a) Correlations between southwest Greenland temperature, T^{SW}, and observed δ versus correlation between T^{SW} and T^{SW}_{pw} calculated by the simplified statistical model, in which $c_{x,W} = 0$ (equation (13)). At the three sites with multiple ice core records, the correlations are shown both for the stack and for the individual records. (b) Same as Figure 6a, but the correlations between T^{SW} and δ have been corrected for the stratigraphic noise in the δ signal using the SNR dependency of latitude shown in Figure 6b (inset).

is calculated at all ice core sites and a comparison with the corresponding values of $c_{T^{SW}_a T^{SW}_{pw}}$ calculated from the simplified statistical model (13) is shown in Figure 6. Using only single cores gives some uncertainty in the estimate of the corrected $c_{\delta,T^{SW}}$, which is apparent by looking at the cores from GRIP and DYE-3. Even so a reasonable agreement between $c_{T^{SW}_a T^{SW}_{pw}}$ and $c_{\delta,T^{SW}}$ is observed, although $c_{T^{SW}_a T^{SW}_{pw}}$ is systematically higher.

[37] A homogeneous $\tilde{\sigma}_\delta$ combined only with information of mean and variability of precipitation seasonality could therefore explain the observed correlation pattern. Accounting also for the correlation between temperature and precipitation seasonality decreases the expected temperature information of northwestern Greenland ice cores even further as was found in section 5.1. However, comparison with the observations from Camp Century and NEEM suggests that this decrease is too large. The correlation between δ values and T^{SW} is found to be reasonably unaffected by high-pass filtering of the records with varying cutoff frequency. This rules out the possibility that the higher correlations to T^{SW} observed in the ice cores are due to low-frequency climate variability not detectable in the short ERA series. A likely explanation is rather that the ERA-40 overestimate $c_{x,W}$ as indicated by coastal observations, but it is also possible that the interannual δ signal prior to the precipitation weighting is relatively stronger in northwestern Greenland.

[38] Precipitation weighting is therefore a strong candidate to explain the gradient of $c_{\delta,T^{SW}}$. The fact that Camp Century is further from the sites of the temperature observations than DYE-3 and Summit is unlikely to explain the low correlation by itself, since the annual temperature signal over Greenland is spatially coherent, indeed in ERA-40 the annual temperatures at Camp Century and southwestern Greenland have a correlation of 0.84. However, different source areas of the precipitation in North Greenland might partly explain the lost connection of the δ signal in this sector with T^{SW}.

6. Seasonally Resolved δ Records

[39] Using again T^{SW}_{pw} as an analogue for δ, we now consider the reconstruction of T_a using only a fraction of each annual layer by applying the analysis of *Vinther et al.* [2010] to synthetic records generated from ERA-40 fields. Using the local daily precipitation data, T^{SW} is put on a synthetic depth scale. Defining midsummer and midwinter markers as local extrema in the record, annual series of precipitation weighted temperature are calculated including only a variable fraction, r, of each annual layer centered on midwinter. For different values of r, the regional signal of the synthetic cores, T_{cores}, is then determined as the first principal component (PC1) of the spatial variability over south and central parts of the ice sheet with an elevation above 1500 meters. The loading patterns of PC1 for the fractions 0.5 and 1 are shown in Figure 7. The correlations of such series of T_{cores} with coastal winter centered time means of temperature are then calculated.

[40] These correlations are shown in Figure 8 as a function of the ice core fractions included. It is seen that this correlation decreases when fractions are increased, even for annual temperatures (August–July). The significance of this decrease has been tested by multiple repetition of the analysis using 44 random years (with replacement). In each such simulation we determine the correlation between annual temperature and T^{SW}_{pw} using a fraction of both $r = 0.5$ and $r = 1$. Figure 8 (inset) shows the resulting distribution of

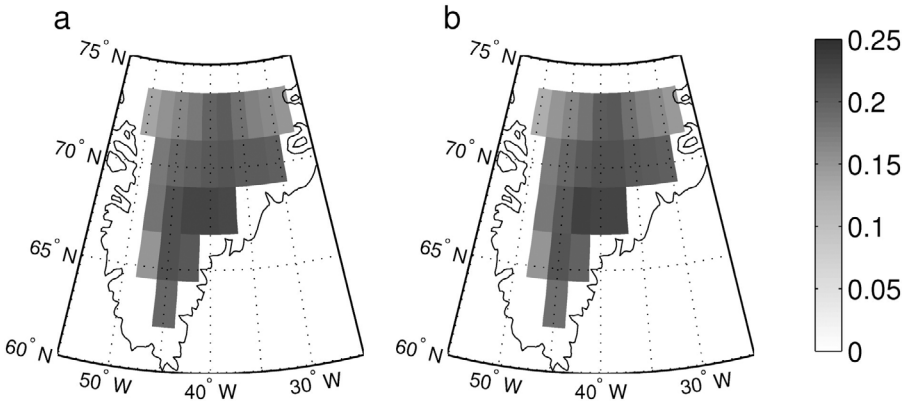

Figure 7. Load patterns for the first principal component of the synthetic ice core signal. The local annual series have been constructed from (a) 50% of each annual layer centered on the winter peak, corresponding to $r = 0.5$, or (b) 100% of each annual layer, corresponding to $r = 1$.

the difference between these two correlation estimates which is greater than zero in 99.95% of the simulations. The uncertainty in the correlation estimate is seen to be of a similar magnitude as the decrease. As just demonstrated the shape of the curve is robust, whereas the uncertainty is mainly associated with its level. A decrease in the correlation is seen between $r = 0.3$ and $r = 0.5$, but such a decrease is not seen in the correlation between the PC1 of the real ice cores and T_a^{SW}. However, using the numerical simulation described above, we find that this decrease in correlation is not significant.

[41] The evolution of $c_{T^{SW},T_{cores}^{SW}}$ with r seen in Figure 8, must originate from local precipitation weighting, since the loading patterns used to generate T_{cores}^{SW} are fairly homogenous and independent of r. The effect can qualitatively be understood in terms of the simplified statistical model for the seasonal precipitation weighting. In the domain where r is sufficiently small to exclude the summer layers, $\tilde{\sigma}_x = 0$. As there is no seasonal scale noise in the precipitation weighting, this implies that $c_{T^{SW},T_{cores}^{SW}}$ is controlled by biasing on the synoptical time scale. In the other domain where r is sufficiently large to include 100% of every winter layer $\tilde{\sigma}_x$ is

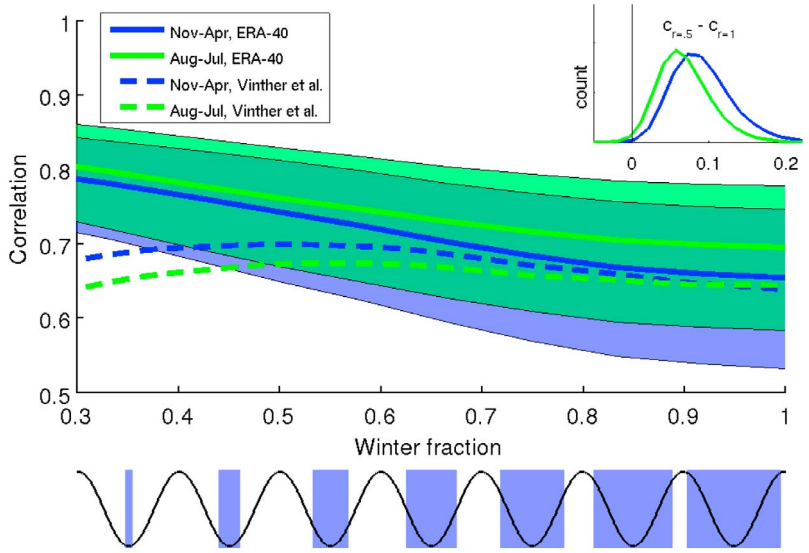

Figure 8. A synthetic ice core is generated at each grid point of ERA-40 in interior southern and central Greenland using daily local precipitation and T^{SW}. Time series of precipitation-weighted mean winter temperature are then computed including only winter layers, which are defined as a variable fraction, r, of annual layers centered on the winter minima (blue boxes). Figure 8 shows the correlation between the first principal component of such precipitation-weighted temperatures, T_{cores}, and that of annual temperature (green) and winter temperature (blue) as a function of r with a 1σ envelope. Even for the annual temperatures this correlation is seen to decrease when r is increased. The histogram (inset) shows the uncertainty in the decrease in the correlation between values of $r = 0.5$ and $r = 1$ as determined by a boot-strapping method. Dashed lines show the similar correlations for the original study by *Vinther et al.* [2010], where T_{cores} was determined from ice core δ values.

nonzero. In the statistical model $\tilde{\sigma}_x$ does not depend on r inside this domain, since excluding a fraction of the annual layers is equivalent to increasing the winter fractions of precipitation, x, by a factor of $1/r$. In order to account for the gradual transition of $c_{T^{SW},T^{SW}_{cores}}$ between $r \sim 0.5$ and $r = 1$ the statistical model would have to be improved with a smoother annual cycle.

7. Conclusions

[42] Based on the subannual climatology of ERA-40, the information about the year-to-year temperature variations contained in Greenland isotope records was found to likely be limited by the seasonal precipitation weighting process for present-day conditions. The seasonal precipitation weighting was analyzed using a simple statistical model and the three terms, which control the correlation between the time and precipitation weighted signal were identified. The measure of the signal strength ($\tilde{\sigma}_W$) is the interannual variability of T, or alternatively δ, which is controlled by the winter value, relative to the amplitude of the annual cycle. Secondly, the precipitation weighting's ability to corrupt the signal ($\tilde{\sigma}_x$) increases with interannual variability of precipitation seasonality. It also increases where, on average, less relative precipitation falls in winter, since the signal is carried with the winter snow. Finally, a correlation between annual excursions of temperature and winter seasonality of precipitation ($c_{x,W}$) can either mask or amplify the temperature signal, depending on its sign.

[43] The low correlation in northwestern Greenland between observed δ and coastal temperatures was found to be in agreement with the spatial pattern of $\tilde{\sigma}_x$ as determined from ERA-40. The value of $c_{x,W}$ in this region, whether calculated from local or southwest Greenland temperature, decreases this correlation even further, although a comparison with coastal observations reveals that this effect may be strongly exaggerated in ERA-40. The observation from ice cores that using only 50% of each annual layer centered on midwinter gave the optimal correlation between δ and T^{SW} was found to be sufficiently explained by the precipitation weighting alone. Following the present analysis, the explanation is not only that the summer snow carries little information about the annual temperature, but furthermore that variable thickness of the summer layer induces significant noise in the δ record.

[44] Some important questions remain to be addressed. Observational constraints on the interannual variability of the precipitation seasonality and its covariance with temperature in interior Greenland are required to reaffirm our conclusions on the impact of precipitation weighting. The analogy between temperature and δ likely has its limitations on the synoptical time scale, but the δ values from a collection of fresh snow and air moisture could help bridge the gap from event to the seasonal time scale. Indeed there is a need for a more explicit modeling of the physical processes controlling the δ signal. The statistical approach of the present study should only be seen as a supplement. However, our results show that any attempt to simulate the interannual δ variability in Greenland must very accurately simulate the precipitation seasonality. Another question not addressed here is to what extent the assumptions of the statistical model are fulfilled under other climatic conditions. For instance may synoptic biasing always be neglected? At the Antarctic Peninsula, the spatial gradient of the correlation between local annual mean and accumulation weighted temperatures seems to be the result of a strong anticorrelation between annual temperature and synoptic biasing in the northern part of the peninsula, so at least in this region synoptic variability must also be accounted for. Further investigations of potential synoptic biasing in Greenland throughout the Holocene are therefore required. Provided these questions can be answered, the Greenland ice cores can provide quantitative information, not only about annual temperatures, but possibly also about the subannual accumulation history.

Appendix A: Correcting $c_{\delta,T^{SW}}$ for Stratigraphic Noise

[45] Where multiple cores are available the correlation between coastal temperature and the local δ signal can to some extent be corrected for the signal loss associated with the redistribution of snow. By splitting the jth record, δ^j, into a common signal part, s, and an independent noise part, η^j.

$$\delta^j = s + \eta^j \tag{A1}$$

and assuming that the noise in each record at the site has equal variance it can be shown that [e.g., *Vinther et al.*, 2006]

$$SNR \equiv \frac{\sigma_s^2}{\sigma_\eta^2} = \frac{\sigma_\Delta^2 - \frac{1}{N}\overline{\sigma_\delta^2}}{\overline{\sigma_\delta^2} - \sigma_\Delta^2} \tag{A2}$$

where Δ is the stack of N cores given by

$$\Delta = \frac{1}{N}\sum_{j=1}^{N} \delta^j \tag{A3}$$

[46] Given the SNR, the correlation between s and T^{SW} can be estimated. Using (A1) and (A3) we find

$$c_{s,T} = \frac{\langle sT \rangle}{\sigma_s \sigma_T} = \frac{\langle \Delta T \rangle}{\sigma_\Delta \sigma_T} \cdot \frac{\sigma_\Delta}{\sigma_s} = c_{\Delta,T} \frac{\left(\sigma_s^2 + \frac{\sigma_\eta^2}{N}\right)^{\frac{1}{2}}}{\sigma_s}$$
$$= c_{\Delta,T}\left(1 + (N \cdot SNR)^{-1}\right)^{\frac{1}{2}} \tag{A4}$$

[47] Performing the analysis where multiple cores are available over the period 1841–1970 AD we find the signal-to-noise ratios in annual resolution to be: 1.5 ± 0.4 at Camp Century, 0.8 ± 0.1 at Summit and 1.6 ± 0.3 at DYE-3 (two cores only). Similar but higher values at Camp Century and DYE-3 were found in a study by *Fisher et al.* [1985]. This study also found low values of SNR at other cores from Central Greenland, namely Milcent and Crete. The generally higher values reported by *Fisher et al.* [1985] compared to the results of the present study can be explained by the diffusion correction applied here. The resulting correlations between δ and T^{SW} are shown in Table A1. Because the SNR is already increased by the stacking, the relatively

Table A1. Stacked δ Records

Location	Cores	SNR	σ_s^2	Correlation		
				T^{SW} and Two Cores[a]	T^{SW} and Δ	T^{SW} and s
Dye-3	5	1.3	0.53	0.53	0.58	0.63
GRIP	6	0.8	0.69	0.47	0.54	0.60
Camp Century	2	1.5	1.23	0.16	0.16	0.19

[a]The mean correlation using all combinations of two-core stacks.

lower correlation found at Camp Century is seen independently of whether the correction (A4) is applied.

Appendix B: Synoptic and Seasonal Precipitation Intermittency

[48] On the Antarctic Peninsula, *Sime et al.* [2009] used ERA-40 reanalysis to evaluate the relative importance of each time scale for the potential of δ to record interannual temperature variability. The following provides a summary of their method:

[49] Daily local temperature and accumulation series from ERA-40 are split into a synoptic band (period < 60 days), seasonal band (60 days < period < 375 days), annual band (period > 375 days) and mean values: $T = \overline{T} + T^{synop} + T^{season} + T^{annual}$ and $p = \overline{p} + p^{synop} + p^{season} + p^{annual}$. The annual mean precipitation-weighted temperature of year a can then be found from expansion of (2), neglecting covariances between different bands

$$T_{pw}(a) \approx T_a(a) + B^{synop}(a) + B^{season}(a), \text{ where for band X}$$
$$B^X(a) \equiv \frac{\sum_a T^X p^X}{\sum_a p} \tag{B1}$$

[50] Here $B^{synop} + B^{season} \equiv B^{subann}$ is the annual difference between T_a and T_{pw}. By considering only one band at a time, its relative importance on the relationship between T_a and T_{pw} can be evaluated. Note that unlike Central Greenland, significant melt occurs on the Antarctic Peninsula, so in the original study accumulation weighted local temperature was used as the analogue to δ.

[51] We apply the analysis of *Sime et al.* [2009] at three sites on the Greenland Ice Sheet to investigate the relative impact of synoptic and seasonal scale effects. Daily surface air temperatures and precipitation sums from the ERA-40 data set have been interpolated (linearly, using the four nearest grid points) to the ice core sites. Table B1 summarizes the correlation between T_a and T_{pw}, where the latter is calculated from either the synoptic (as $T_a + B^{synop}$), the seasonal or both the subannual bands. At all sites a high correlation between T_a and the synoptically weighted temperature is found. Although the synoptic weighting decreases the gradient of T_a vs. T_{pw} slightly at DYE-3 and GRIP, the correlation is largely controlled by the seasonal scale.

[52] The annual mean and precipitation weighted annual mean temperatures have also been calculated directly using equations (1) and (2). This has been done year by year (summer to summer) for the period 1958–2002 giving 44 points. The correlation between T_a and T_{pw} is for the three Greenland sites: DYE-3 0.58 ± 0.12, GRIP 0.27 ± 0.14 and Camp Century −0.06 ± 0.15. Note (except at Camp Century) that these numbers are lower than the corresponding correlations between T_a and $T_a + B^{synop} + B^{season}$ shown in Table B1. This is because (B1) neglects the considerable variability of the biasing caused together by p^{annual} and T^{season} due to the 1 year window size. The method of *Sime et al.* [2009] therefore underestimates the effect of the seasonal weighting for Greenland conditions, but it remains a useful tool for separating the importance of synoptic and seasonal precipitation weighting.

Appendix C: Model Details

[53] The means of T_{pw} and T_a are given as

$$\overline{T_{pw}} = \overline{xW} + (1-\bar{x})S \equiv \bar{x}\overline{W} + \sigma_{x,W} + (1-\bar{x})S \tag{C1}$$

$$\overline{T_a} = \beta\overline{W} + (1-\beta)S \tag{C2}$$

so subtracting the means from (4) and (5) gives

$$T'_{pw,i} = x_i W_i - \bar{x}\overline{W} - \sigma_{x,W} - x'_i S \tag{C3}$$

$$T'_{a,i} = \beta W'_i \tag{C4}$$

with primes denoting deviations from the mean values, which are denoted with bars. $\sigma_{x,W}$ is the covariance of x and W. To calculate the variance and covariance terms of T_a and T_{pw} from (C3) and (C4) the following is assumed: W' has a symmetric distribution and x depends on W as $x_i = aW_i + b + \eta_i$. The noise, η, is only required to have a defined second moment and to be uncorrelated with W. With these assumptions we get after some calculations

$$\overline{T'_{a,i}T'_{pw,i}} = \beta\left(\bar{x}\sigma_W^2 - \sigma_{x,W}\left(S - \overline{W}\right)\right) \tag{C5}$$

$$\overline{T'^2_{a,i}} = \beta^2\sigma_W^2 \tag{C6}$$

$$\overline{T'^2_{pw,i}} = \bar{x}^2\sigma_W^2 + \left(S-\overline{W}\right)^2\sigma_x^2 - 2\sigma_{x,W}\bar{x}\left(S-\overline{W}\right) + \sigma_x^2\sigma_W^2\left(1 + c_{x,W}^2\left(\frac{\overline{W'^4}}{\sigma_W^4} - 2\right)\right) \tag{C7}$$

Here $c_{x,W}$ is the coefficient of linear correlation between x and W. The last term in (C7) represents a higher-order

Table B1. Correlation and Gradient Between Local Annual Temperature and Precipitation-Weighted Temperatures for Different Bands

Location	Correlation			Gradient		
	T_a and $T_a + B_p^{synop}$	T_a and $T_a + B_p^{season}$	T_a and $T_a + B_p^{subann}$	T_a Versus $T_a + B_p^{synop}$	T_a Versus $T_a + B_p^{season}$	T_a Versus $T_a + B_p^{subann}$
Dye-3	0.82	0.80	0.76	0.82	1.11	0.93
GRIP	0.87	0.61	0.51	0.77	0.85	0.63
Camp Century	0.76	−0.06	0.07	1.25	−0.12	0.13

correction that only becomes important when the fluctuations of $S - W_i$ and x_i become comparable to or larger than their mean values. We discard the last term as ERA-40 outputs show that it is nearly two orders of magnitude smaller than the sum of the other terms all over Greenland.

[54] **Acknowledgments.** The authors thank the Danish National Research Foundation for the financial support that made this study possible. The authors would also like to thank ECMWF for producing and making available the ERA-40 reanalysis data as well as Jesper Sjolte for providing access to his model data ($REMO_{iso}$). Finally, we thank the reviewers for their many constructive comments and suggestions.

References

Andersen, K. K., P. D. Ditlevsen, S. O. Rasmussen, H. B. Clausen, B. M. Vinther, S. J. Johnsen, and J. P. Steffensen (2006), Retrieving a common accumulation record from Greenland ice cores for the past 1800 years, *J. Geophys. Res.*, *111*, D15106, doi:10.1029/2005JD006765.

Barlow, L. K., J. W. C. White, R. G. Barry, J. C. Rogers, and P. M. Grootes (1993), The North Atlantic Oscillation signature in deuterium and deuterium excess signals in the Greenland Ice Sheet Project 2 Ice Core, 1840–1970, *Geophys. Res. Lett.*, *20*(24), 2901–2904, doi:10.1029/93GL03305.

Bromwich, D. H., R. L. Fogt, K. I. Hodges, and J. E. Walsh (2007), A tropospheric assessment of the ERA-40, NCEP, and JRA-25 global reanalyses in the polar regions, *J. Geophys. Res.*, *112*, D10111, doi:10.1029/2006JD007859.

Cappelen, J., E. V. Laursen, P. V. Jørgensen, and C. Kern-Hansen (2008), DMI monthly climate data collection 1768–2007, Denmark, the Faroe Islands and Greenland, *Tech. Rep. 08-04*, 53 pp., Dan. Meteorol. Inst., Copenhagen.

Capron, E., et al. (2010), Millennial and sub-millennial scale climatic variations recorded in polar ice cores over the last glacial period, *Clim. Past*, *6*(3), 135–183, doi:10.5194/cp-6-345-2010.

Ciais, P., and J. Jouzel (1994), Deuterium and oxygen 18 in precipitation: Isotopic model, including mixed cloud processes, *J. Geophys. Res.*, *99*(D8), 16,793–16,803, doi:10.1029/94JD00412.

Clausen, H. B., and C. U. Hammer (1988), The Laki and Tambora eruptions as revealed in Greenland ice cores from 11 locations, *Ann. Glaciol.*, *10*, 16–22.

Cuffey, K. M., and G. D. Clow (1997), Temperature, accumulation, and ice sheet elevation in central Greenland through the last deglacial transition, *J. Geophys. Res.*, *102*(C12), 26,383–26,396, doi:10.1029/96JC03981.

Dansgaard, W. (1964), Stable isotopes in precipitation, *Tellus*, *16*(4), 436–468.

Fisher, D. A., N. Reeh, and H. B. Clausen (1985), Stratigraphic noise in time series derived from ice cores, *Ann. Glaciol.*, *7*, 76–83.

Hanna, E., J. McConnell, S. Das, J. Cappelen, and A. Stephens (2006), Observed and modeled Greenland ice sheet snow accumulation, 1958–2003, and links with regional climate forcing, *J. Clim.*, *19*(3), 344–358, doi:10.1175/JCLI3615.1.

Hoffmann, G., M. Werner, and M. Heimann (1998), Water isotope module of the ECHAM atmospheric general circulation model: A study on timescales from days to several years, *J. Geophys. Res.*, *103*(D14), 16,871–16,896, doi:10.1029/98JD00423.

Johnsen, S. J. (1977), Stable isotope profiles compared with temperature profiles in firn with historical temperature records, in *Isotopes and Impurities in Snow and Ice Symposium: Proceedings of the Grenoble Symposium, August–September 1975*, IAHS AISH Publ., *118*, 388–392.

Johnsen, S. J., H. B. Clausen, K. M. Cuffey, G. Hoffmann, J. Schwander, and T. Creyts (2000), Diffusion of stable isotopes in polar firn and ice: The isotope effect in firn diffusion, in *Physics of Ice Core Records*, vol. 159, edited by T. Hondoh, pp. 121–140, Hokkaido Univ. Press, Sapporo, Japan.

Langen, P. L., and B. M. Vinther (2009), Response in atmospheric circulation and sources of Greenland precipitation to glacial boundary conditions, *Clim. Dyn.*, *32*(7–8), 1035–1054.

Masson-Delmotte, V., et al. (2005), Holocene climatic changes in Greenland: Different deuterium excess signals at Greenland Ice Core Project (GRIP) and NorthGRIP, *J. Geophys. Res.*, *110*, D14102, doi:10.1029/2004JD005575.

Rogers, J. C., J. F. Bolzan, and V. A. Pohjola (1998), Atmospheric circulation variability associated with shallow-core seasonal isotopic extremes near Summit, Greenland, *J. Geophys. Res.*, *103*(D10), 11,205–11,219, doi:10.1029/98JD02618.

Schneider, D. P., and D. C. Noone (2007), Spatial covariance of water isotope records in a global network of ice cores spanning twentieth-century climate change, *J. Geophys. Res.*, *112*, D18105, doi:10.1029/2007JD008652.

Schneider, D. P., E. J. Steig, and T. Van Ommen (2005), High-resolution ice-core stable-isotopic records from Antarctica: Towards interannual climate reconstruction, *Ann. Glaciol.*, *41*, 63–70.

Schuenemann, K. C., and J. J. Cassano (2009), Changes in synoptic weather patterns and Greenland precipitation in the 20th and 21st centuries, Part 1: Evaluation of late 20th century simulations from IPCC models, *J. Geophys. Res.*, *114*, D20113, doi:10.1029/2009JD011705.

Schuenemann, K. C., J. J. Cassano, and J. Finnis (2009), Synoptic forcing of precipitation over Greenland: Climatology for 1961–99, *J. Hydrometeorol.*, *10*, 60–78, doi:10.1175/2008JHM1014.1.

Sime, L. C., J. C. Tindall, E. W. Wolff, W. M. Connolley, and P. J. Valdes (2008), Antarctic isotopic thermometer during a CO_2 forced warming event, *J. Geophys. Res.*, *113*, D24119, doi:10.1029/2008JD010395.

Sime, L. C., G. J. Marshall, R. Mulvaney, and E. R. Thomas (2009), Interpreting temperature information from ice cores along the Antarctic Peninsula: ERA-40 analysis, *Geophys. Res. Lett.*, *36*, L18801, doi:10.1029/2009GL038982.

Sjolte, J., G. Hoffmann, S. J. Johnsen, B. M. Vinther, V. Masson-Delmotte, and C. Sturm (2011), Modeling the water isotopes in Greenland precipitation 1959–2001 with the meso-scale model REMO-iso, *J. Geophys. Res.*, *116*, D18105, doi:10.1029/2010JD015287.

Sodemann, H., C. Schwierz, and H. Wernli (2008a), Interannual variability of Greenland winter precipitation sources: Lagrangian moisture diagnostic and North Atlantic Oscillation influence, *J. Geophys. Res.*, *113*, D03107, doi:10.1029/2007JD008503.

Sodemann, H., V. Masson-Delmotte, C. Schwierz, B. M. Vinther, and H. Wernli (2008b), Interannual variability of Greenland winter precipitation sources: 2. Effects of North Atlantic Oscillation variability on stable isotopes in precipitation, *J. Geophys. Res.*, *113*, D12111, doi:10.1029/2007JD009416.

Steen-Larsen, H. C., et al. (2011), Understanding the climatic signal in the water stable isotope records from the NEEM shallow firn/ice cores in northwest Greenland, *J. Geophys. Res.*, *116*, D06108, doi:10.1029/2010JD014311.

Steffensen, J. P. (1985), Microparticles in snow from the south Greenland ice sheet, *Tellus, Ser. B*, *37*(4–5), 286–295, doi:10.1111/j.1600-0889.1985.tb00076.x.

Steig, E. J., P. M. Grootes, and M. Stuiver (1994), Seasonal precipitation timing and ice core records, *Science*, *266*, 1885–1886.

Town, M. S., S. G. Warren, V. P. Walden, and E. D. Waddington (2008), Effect of atmospheric water vapor on modification of stable isotopes in near-surface snow on ice sheets, *J. Geophys. Res.*, *113*, D24303, doi:10.1029/2008JD009852.

Uppala, S. M., et al. (2005), The ERA-40 re-analysis, *Q. J. R. Meteorol. Soc.*, *131*(612), 2961–3012, doi:10.1256/qj.04.176.

Vinther, B. M. (2003), Seasonal $\delta^{18}O$ signals in Greenland ice cores, M.S. thesis, Dep. of Geophys., Niels Bohr Inst. for Astron., Phys., and Geophys., Univ. of Copenhagen, Copenhagen.

Vinther, B., K. Andersen, P. Jones, K. Briffa, and J. Cappelen (2006), Extending Greenland temperature records into the late eighteenth century, *J. Geophys. Res.*, *111*, D11105, doi:10.1029/2005JD006810.

Vinther, B. M., et al. (2006), A synchronized dating of three Greenland ice cores throughout the Holocene, *J. Geophys. Res.*, *111*, D13102, doi:10.1029/2005JD006921.

Vinther, B. M., P. D. Jones, K. R. Briffa, H. B. Clausen, K. K. Andersen, D. Dahl-Jensen, and S. J. Johnsen (2010), Climatic signals in multiple highly resolved stable isotope records from Greenland, *Quat. Sci. Rev.*, *29*, 522–538,doi:10.1016/j.quascirev.2009.11.00.

von Storch, H., H. Langenberg, and F. Feser (2000), A spectral nudging technique for dynamical downscaling purposes, *Mon. Weather Rev.*, *128*(10), 3664–3673.

Werner, M., and M. Heimann (2002), Modeling interannual variability of water isotopes in Greenland and Antarctica, *J. Geophys. Res.*, *107*(D1), 4001, doi:10.1029/2001JD900253.

Werner, M., U. Mikolajewicz, M. Heimann, and G. Hoffman (2000), Borehole versus isotope temperatures on Greenland: Seasonality does matter, *Geophys. Res. Lett.*, *27*(5), 723–726, doi:10.1029/1999GL006075.

White, J. W. C., L. K. Barlow, D. Fisher, P. Grootes, J. Jouzel, S. F. Johnsen, M. Stuiver, and H. B. Clausen (1997), The climate signal in the stable isotopes of snow from Summit, Greenland: Results of comparisons with modern climate observations, *J. Geophys. Res.*, *102*(C12), 26,425–26,439, doi:10.1029/97JC00162.

P. Ditlevsen, P. L. Langen, A. Persson, and B. M. Vinther, Centre for Ice and Climate, Niels Bohr Institute, University of Copenhagen, Juliane Maries Vej 30, DK-2100 Copenhagen, Denmark. (asbjrn@nbi.ku.dk; bo@gfy.ku.dk)